Construction and Building Materials 451 (2024) 138795

Contents lists available at ScienceDirect

Construction and Building Materials

journal homepage: www.elsevier.com/locate/conbuildmat

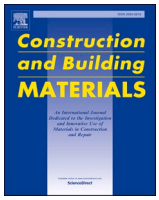

# Effect of lignin on veneer densification and set-recovery

Catherine Kilumets [a], Heikko Kallakas [a], Sally Ralph [b], J.Y. Zhu [b], Christopher G. Hunt [b], Anti Rohumaa [a,c,*], Jaan Kers [a]

[a] Laboratory of Wood Technology, Department of Material and Environmental Technology, Tallinn University of Technology, Tallinn 19086, Estonia
[b] USDA Forest Service, Forest Products Laboratory, Madison, WI 53726, USA
[c] FiberLaboratory, South-Eastern Finland University of Applied Sciences, Vipusenkatu 10, Savonlinna FI-57200, Finland

ARTICLE INFO

*Keywords:*
Wood densification
Delignification
Set-recovery
Thickness swelling
Dimensional stability
Veneer

ABSTRACT

Wood densification, aimed at enhancing mechanical properties through compression, faces challenges due to set-recovery, where densified wood regains its original shape upon re-moistening. However, understanding the role of lignin in set-recovery remains elusive. In this study, acidified sodium chlorite was applied to achieve approximately 50 % delignification without removing other wood components from 3.2 mm veneers of birch, aspen, and grey alder. The veneers were then densified at 100°C and 6 MPa, with wood moisture contents (MC) of 10 % and 16 %. The morphology, physical properties, and dimensional stability of densified wood are studied in relation to delignification and MC at densification. Delignification with subsequent densification at 16 % MC was better than at 10 % MC, increasing the resultant wood density by 89 %, 148 %, and 146 % for birch, aspen, and grey alder, respectively. In general, delignification and higher moisture content during compression resulted in better compression ratios and lower set recovery. This delignification-densification approach reduced set-recovery across all wood species to a range of 71–86 %, suggesting that under these conditions, lignin has only a marginal impact on shape memory and unrestrained set-recovery in wood. Therefore, cellulose microfibrils are likely playing a dominant role.

## 1. Introduction

Wood density significantly influences mechanical properties [1,2]. Wood densification is aimed at reducing wood porosity through compression to improve wood surface hardness, abrasion resistance, and transverse shear strength [2]. This process has generated strong interest as it has the potential to improve the properties of low-density wood species, making them suitable for high-end applications such as wooden flooring [3] and higher-value veneer-based composite materials for construction [4]. However, due to wood's hygroscopic nature, densified material can regain its original shape when re-moistened, a phenomenon known as set-recovery [2] which greatly cancels out the benefits of wood densification.

To address the set-recovery issue after wood densification and retain the desired gains in wood mechanical properties, literature work on fixing wood deformation can provide some guides. For example, chemical treatments such as acetylation [5], maleic acid glycerol [6], ionic liquids [7] or impregnation with an unpolymerized low molecular weight resin such as phenol-formaldehyde to cure during densification [8,9] have been utilized to fix wood in position. However, these solutions are costly. One promising approach developed recently is using deep eutectic solvents (DES), which have shown potential in shape-fixation [10]. Thermal treatment does not use chemicals and can increase wood's dimensional stability and its resistance to decay [11]. Typical treatment temperatures range from 160°C to 250°C with holding times of several hours [8,12]. Applying steam can shorten the holding time to a few minutes (e.g., from 180°C for 20 h to 180°C for 8 min), which increases throughput and saves energy [13]. Although using higher temperatures in treatments can decrease set-recovery, treatments above 160°C–180°C decrease wood's mechanical properties, particularly toughness. These changes are especially pronounced under dry heating conditions [2,8,13].

The objective of the present study is to develop some fundamental understanding on set recovery after wood densification. With the combination of moisture, temperature, and compression, all constituents of wood, except crystalline cellulose, deform plastically during

* Corresponding author at: Laboratory of Wood Technology, Department of Material and Environmental Technology, Tallinn University of Technology, Tallinn 19086, Estonia.
*E-mail address:* anti.rohumaa@xamk.fi (A. Rohumaa).

https://doi.org/10.1016/j.conbuildmat.2024.138795
Received 17 May 2024; Received in revised form 11 October 2024; Accepted 16 October 2024

densification. The cellulose microfibrils, containing crystalline and noncrystalline regions, undergo elastic deformation to result in stored elastic strain energy. The formation of hydrogen bonds between cellulose and hemicelluloses upon drying and the presence of lignin contribute to temporarily fixing wood deformation. When water is attracted to the polar hydroxyl groups in cellulose, hemicelluloses, and lignin, it breaks hydrogen bonds in all three polymers [8,14]. The stored elastic energy can then overcome the plasticized components, pushing the wood back toward its original shape – set-recovery. During thermal modification, the most hygroscopic component of wood, hemicelluloses, are also the most heat-sensitive. The number of hydroxyl groups decreases as hemicelluloses begin to break down [11,15]. The degradation of C═O groups connected to the aromatic skeleton of lignin also reduces hygroscopicity [16]. This lessens the wood's ability to absorb moisture and plasticize, which could keep the internal stresses locked in place. Research by Higashihara et al. [17] indicates that the dominant mechanism for fixation is polymer rearrangement, resulting in the release of stresses stored in the cell wall during deformation. This release includes the elastic strain energy stored in helical semicrystalline microfibrils, as well as the thermoplastic flow of lignin [2]. Additionally, the loss of lignin-hemicellulose linkages in microfibrils during thermal modification has been found to release stress and create more void space for microfibril rearrangement [2,13]. Furthermore, the application of steam facilitates the relaxation of the lignin-hemicellulose matrix, allowing microfibrils to move more freely within the softened matrix [13]. These insights suggest that set-recovery stems not only from the elasticity and composition of wood components but also from the hydrophobization of the cell wall and stress relaxation [10,16]. Nevertheless, it has remained uncertain whether semicrystalline cellulose or lignin exerts a greater influence on permanent fixation in native wood.

Here, we are trying to focus on one variable, i.e., lignin, at a time, to gain a better understanding of the role of lignin contributing to set-recovery. Smaller quantities of lignin are hypothesized to contribute little to the shape memory effect simply because the smaller quantity of lignin is insufficient to store significant internal stresses. Our aim is to reduce the accumulation of internal stresses during densification, thereby gaining a greater understanding of the role that lignin plays in set-recovery by partially dissolving lignin from native wood specimens (NW). The acid chlorite treatment used is known for dissolving lignin without impacting hemicelluloses. Because lignin has a complex chemical structure with different functional groups of varying degrees of polarity, it has both hydrophobic and hydrophilic elements [18]. The free hydroxyl group in lignin is capable of hydrogen bonding [19]. It was observed that the nanoindentation in the middle lamella fully recovered after being wetted [20]. This observation meant that a good shape memory material can be made from lignin and hemicelluloses. Hemicelluloses are responsible for reversible swelling while lignin is primarily responsible for remembering the original form [20]. It is possible to lessen set-recovery by compressing wood in a manner that allows lignin to flow to ease internal stresses. By pressing under high temperatures and moisture conditions, wood generally does not swell back to its original, uncompressed state because both heat and moisture act as plasticizers [8,21]. Wood components are quite stable below 100°C above which wood polysaccharides start to depolymerize [22]. Therefore, this study used higher moisture contents while keeping the temperature low (100°C) to allow short press times without steam explosion taking place upon press opening. The Kwei model [23] suggests that wood moisture content affects the glass transition temperature (Tg) of lignin. The *in situ* Tg of lignin is 200°C and 60°C at the moisture content of 0 % and 30 %, respectively [24,25]. As a result, the amorphous lignin can be changed from a glassy to a rubbery state at the testing conditions designed in the present study. The changes in morphological structure, physical properties, and dimensional stability of DW and DL-DW birch (*Betula pendula* Roth), aspen (*Populus tremula* L.), and grey alder (*Alnus incana*) were investigated.

## 2. Materials and methods

### 2.1. Veneer preparation

Three different wood species were used: birch (*Betula pendula* Roth, density of 586 kg/m$^3$), aspen (*Populus tremula* L., 472 kg/m$^3$), and grey alder (*Alnus incana*, 451 kg/m$^3$). All logs were felled in October 2022 at Järvselja, Tartu County, Estonia, Järvselja Learning and Experimental Forest Foundation. The provisioning data showed that the average stand age was 59, 26, and 66 years for birch, grey alder, and aspen. Average diameters were 17, 27, and 27 cm for grey alder, birch, and aspen respectively. The veneer rotary-peeling procedure was derived from Kallakas et al. [26]. After being cut into 1.3-meter-long peeler blocks, logs were immersed in a water bath at 40°C for 72 hours. The peeler blocks were then debarked with a draw knife and rotary peeled into 3.34 mm-thick green veneer using an industrial-sized peeling lathe (Model 3HV66; Raute Oyj, Lahti, Finland). The peeling speed was 60 m/min, the knife sharpening angle 19°, and the compression rate 7 %. The veneer mat was then cut into sheets with dimensions of 900 mm by 400 mm using the pneumatic guillotine (Wärtsilä Corporation, Finland). Veneer sheets were dried in a laboratory-scale veneer dryer (Raute Oyj, Lahti, Finland) at 170 °C. After drying, the veneers were cut into 50×50 mm specimens for further testing.

### 2.2. Delignification

For delignifying the veneers, acidified sodium chlorite treatment was applied by modifying the procedure of Ahlgren and Goring [27] to fit the need for the thicker veneers used in the present study. The chemical charge was 0.3 g sodium chlorite (7758–19–2, Aldrich Chemical Company, Inc., US) and 0.1 ml glacial acetic acid (64–19–7, Fischer Scientific, US) per g of oven-dried (OD) wood. The water-to-wood ratio (w/w) was 15:1. Batches of 50×50 mm veneer samples (NW) were treated in glass desiccators for 6 days at ambient conditions of 20°C, 50 % RH. A fresh charge of chemicals was added without the withdrawal of any solution at 24-hour intervals. After delignification, the samples (DL-W) were soaked in distilled water several times until the water stayed colorless. Washed samples were then dried in an oven at 80°C until constant mass. Solids yield was calculated by Eq. 1.

$$S_y(\%) = \frac{m_1}{m_0} \times 100 \quad (1)$$

where $m_0$ is the initial wood oven-dry (OD) mass and $m_1$ is the delignified wood OD mass.

### 2.3. Densification

To determine the impact of bound water on densification, water vapor uptake was applied to NW and DL-W samples in two separate conditions: 25°C, 65 % RH, and 25°C, 90 % RH. This resulted in a moisture content of ~10 and ~16 %, respectively. The conditioned samples were densified in a radial direction using a hydraulic press (CARVER, Inc., US). Densification was carried out in two steps: preheating the sample to the target of 100°C without pressure for 3 minutes and then densifying at 100°C, 6 MPa for 15 min. After densification, the densified veneer pieces (DW and DL-DW) were oven-dried at 80°C until equilibrium was reached. The compression ratio was calculated using Eq. 2.

$$CR(\%) = \frac{T_o - T_d}{T_o} \times 100 \quad (2)$$

where $T_o$ and $T_d$ are oven-dried thicknesses before and after densification.

**Table 1**
Chemical composition of the specimens (standard deviations shown in parenthesis).

| Species | Sample type | Solids yield (wt%) | Cellulose (wt%) | Hemicelluloses (wt%) | Lignin (wt%) | Density (kg/m$^3$) |
|---|---|---|---|---|---|---|
| Birch | NW | 100.0 | 40.8 (1.3) | 24.3 (0.9) | 25.9 (0.6) | 592.7 (15.9) |
| | DL-W | 89.6 (0.8) | 43.7 (1.5) | 26.5 (0.8) | 14.0 (1.8) | 572.1 (19.6) |
| Aspen | NW | 100.0 | 47.9 (1.1) | 21.4 (1.7) | 23.7 (0.8) | 440.9 (23.5) |
| | DL-W | 89.2 (0.8) | 51.3 (2.3) | 22.5 (0.7) | 12.1 (2.4) | 431.5 (18.9) |
| Grey alder | NW | 100.0 | 40.9 (4.1) | 22.8 (1.1) | 27.6 (0.3) | 436.8 (11.4) |
| | DL-W | 86.0 (0.8) | 44.9 (1.5) | 24.9 (0.9) | 14.9 (1.3) | 401.6 (15.5) |

### 2.4. Chemical composition

Wood chemical composition was analyzed by following the National Renewable Energy Laboratory (NREL) procedure [28]. The Dionex ICS 3000 IC system equipped with a pulsed amperometric detector and a CarboPac PA1 (4 ×250 mm) column was used to analyze wood carbohydrates. The chromatography procedure used to resolve the wood carbohydrates was discussed by Davis [29]. The loss of components was calculated by Eq. 3.

$$Loss_{component}(\%) = \left(1 - \frac{C_1 \times S_y}{C_0}\right) \times 100 \quad (3)$$

where $C_0$ and $C_1$ are the contents of the wood component (%wt) of the undelignified and delignified solids, and $S_y$ is the wood solids yield from delignification obtained using Eq. 1.

### 2.5. Density

Densities of densified and non-densified OD veneers were determined using 50×50 mm specimens. Before measuring, the pieces were dried in an oven at 103°C until constant mass. The ratio between dry weight and volume was calculated using Eq. 4 (ISO 13061–2:2014).

$$\rho = \frac{m}{V} \quad (4)$$

Where m is the oven-dried weight and V is the oven-dried volume of the specimen.

### 2.6. Micromorphology analysis

For light microscopy (LM), reference and densified veneer samples were cut from the middle to observe their microstructures. To preserve the shape of the compressed cells, the transverse surface of the veneer was polished using sanding paper of 1000 grit. The micrographs of cross sections were visualized using a stereoscope (Leica, Germany) equipped with a digital camera (Flea 3, FLIR System, US).

### 2.7. Dimensional stability

Thickness swelling and set-recovery were determined with a 25×25 mm densified wood sample using Eq. 5 [30] and 6 [13], respectively. To reflect end-user conditions, specimens were subjected to two distinct environments: a water soaking for 24 hours to determine the maximum recovery and a humidity condition at 25°C and 65 % RH to obtain a more realistic recovery. The samples were then dried at 80°C until equilibrium. The thicknesses before and after the tests were recorded.

$$TS(\%) = \frac{T_{max} - T_d}{T_d} \times 100 \quad (5)$$

where $T_d$ is the oven-dried thickness after densification and $T_{max}$ is the thickness after water saturation or humid conditions.

$$SR(\%) = \frac{T_r - T_d}{T_o - T_d} \quad (6)$$

where $T_r$ is the recovered thickness after soaking and oven-drying, $T_d$ is the oven-dried thickness after densification and $T_o$ is the oven-dried original thickness before densification. SR = 100 % indicates that the sample thickness was the same after water exposure as before densification.

### 2.8. Data analysis

For the analysis, one-way ANOVA was used to identify variables contributing to significant differences, with an alpha of 0.05. When the p-value was significant, Tukey's post hoc test was used to identify the impact of different treatment levels ($p < 0.05$).

## 3. Results and discussion

### 3.1. Effect of delignification on wood chemical composition

Wood solids yield from delignification ranged from approximately

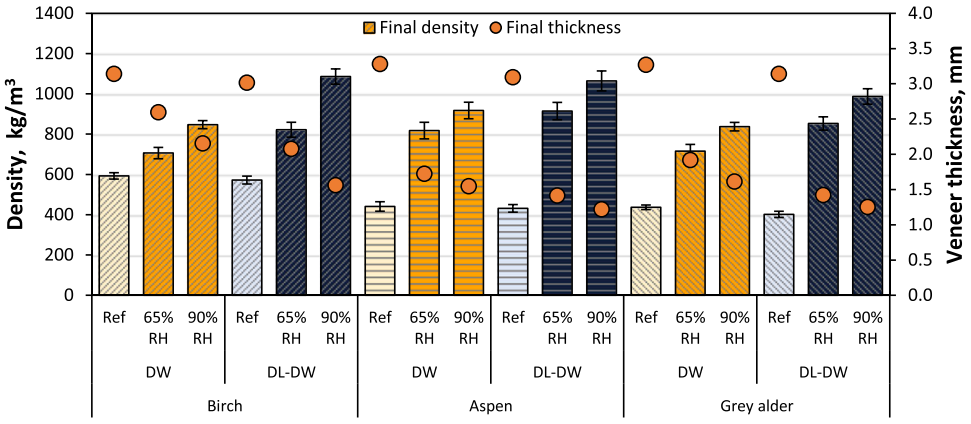


**Fig. 1.** Average (n=10) wood veneer density values and their corresponding thicknesses for DW and DL-DW (at 65 % and 90 % RH) samples. Reference refers to undensified wood.

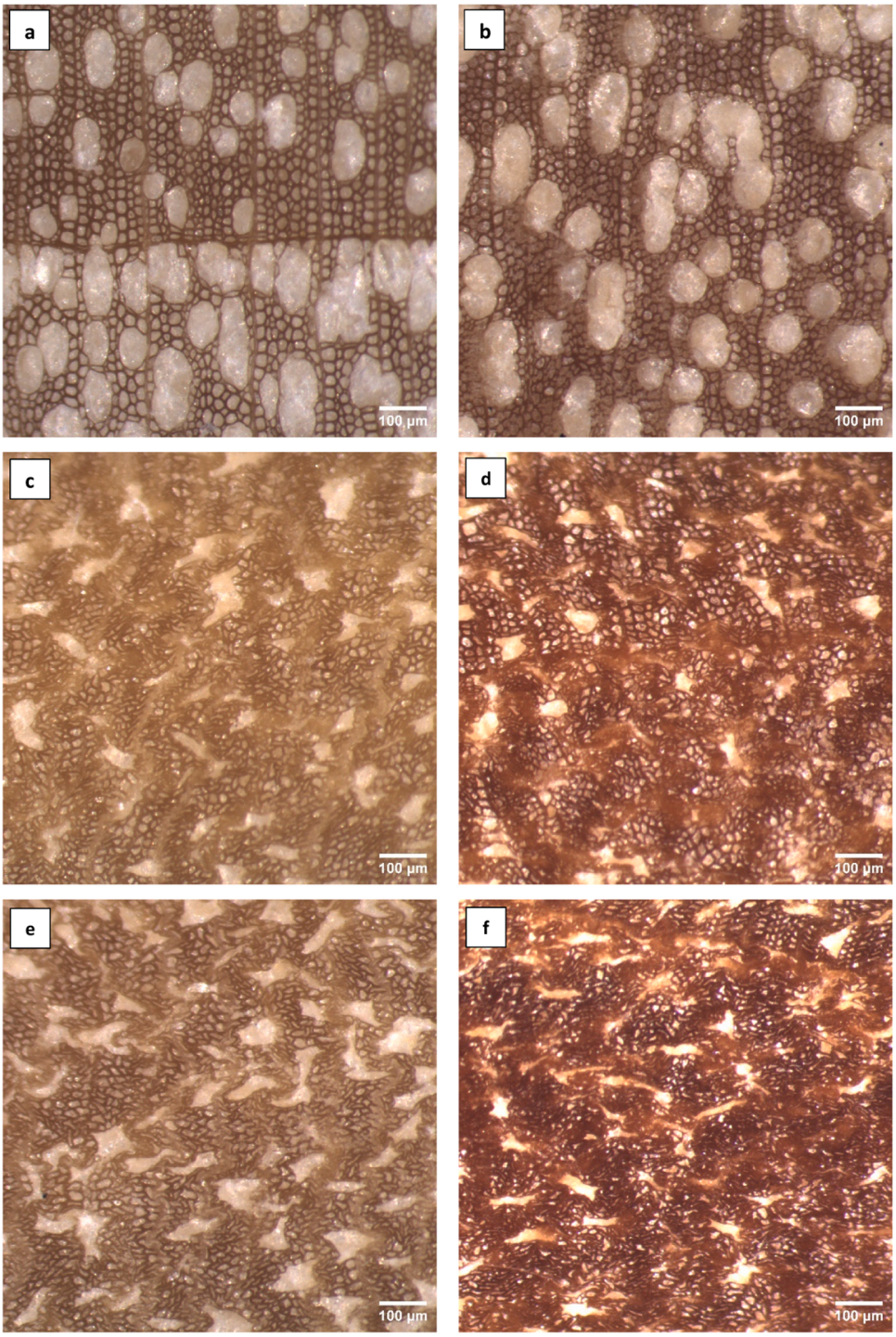


**Fig. 2.** Aspen micrographs of reference and densified specimen: **a** - NW; **b** – DL-W; **c** – DW, densified 65 % RH; **d** – DL-DW, densified 65 % RH; **e** – DW, densified 90 % RH; **f** – DL-DW, densified 90 % RH.

86–90 %, while lignin removal ranged from 51 % to 54 % (Table 1). According to Song et al. [31] densified wood with approximately 45 % lignin removal by alkaline sulfite delignification was shown to have the highest density, strength, and toughness. Alkaline sulfite treatment not only removed lignin but also significantly dissolved hemicelluloses. Our data, however, clearly shows that chlorite treatment preserves hemicelluloses and cellulose well, with losses of only approximately 5 % and 4 %, respectively. Wood density was decreased by 2–8 % because delignification increased the specimens' porosity.

### 3.2. Effects of delignification on wood densification

For undelignified-densified (DW) samples, the highest compression ratio (CR) was 52 % from aspen conditioned at 25°C, 90 % RH resulting in a density increase from 440 to 917 kg/m$^3$ (Fig. 1). Despite grey alder having a similar density to aspen before densification, the difference in wood species led to a slightly lower CR of 50 % with a density of 837 kg/m$^3$ ($p < 0.001$). Overall, densification at 90 % RH (DW) led to an increase in final density by 42 % for birch, 112 % for aspen, and 114 % for grey alder. When delignification was performed before densification

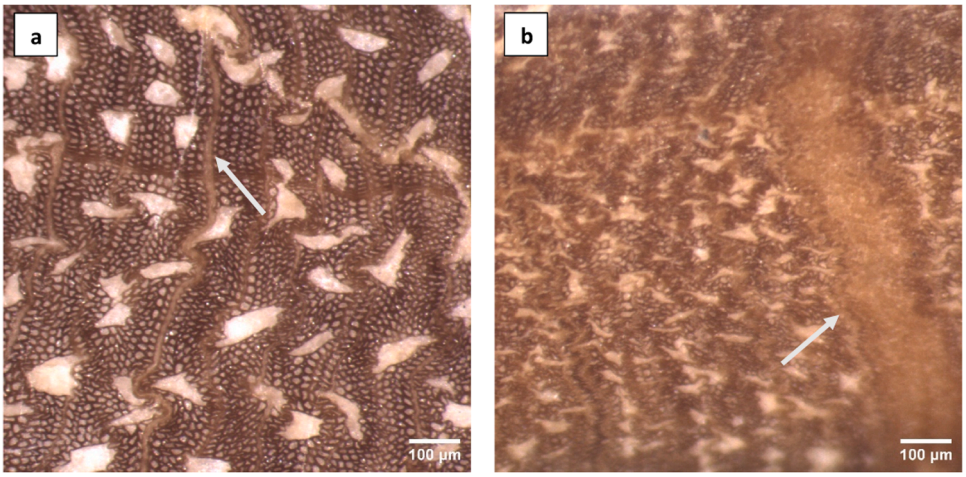


**Fig. 3.** The influence of ray prominence in densification: **a** – birch, DW, densified 90 % RH; **b** – grey alder, DL-DW, densified 65 % RH.

under the same conditions (DL-DW), the final density increased more significantly, by 89 %, 148 %, and 146 % for birch, aspen, and grey alder, respectively ($p < 0.001$). Shams et al. [32] has found that delignification reduced the cell wall's Young's modulus and transverse rigidity. The lower stiffness of delignified walls should facilitate cell collapse during densification. Shear stiffness is also reported to be reduced by lignin removal, thus enabling shear deformation, facilitated by molecular chain slippage [33,34]. These effects can both result in higher density and CR. The greatest density obtained through delignification and densification (DL-DW) was from birch (conditioned at 90 % RH) at 1086 ± 38 kg/m$^3$. As birch is naturally denser wood, its thicker cell walls are less prone to deformation due to higher stiffness [35], resulting in a lower CR of 48 %. Lower density species, however, such as aspen and grey alder exhibited a greater increase in density with a CR of around 60 % under the same experimental conditions. Aspen is particularly noteworthy with the final density of 1064 ± 50 kg/m$^3$, comparable to densified birch ($p = 0.99$).

Subsequently, we investigated the impact of densification conditions. After densifying the specimen under two different wood moisture contents (MC), the differences in CR (i.e. thickness change) and density are evident (Fig. 1). Raising the RH from 65 % to 90 % increased final density and decreased final thickness. When compressed at 90 % RH,

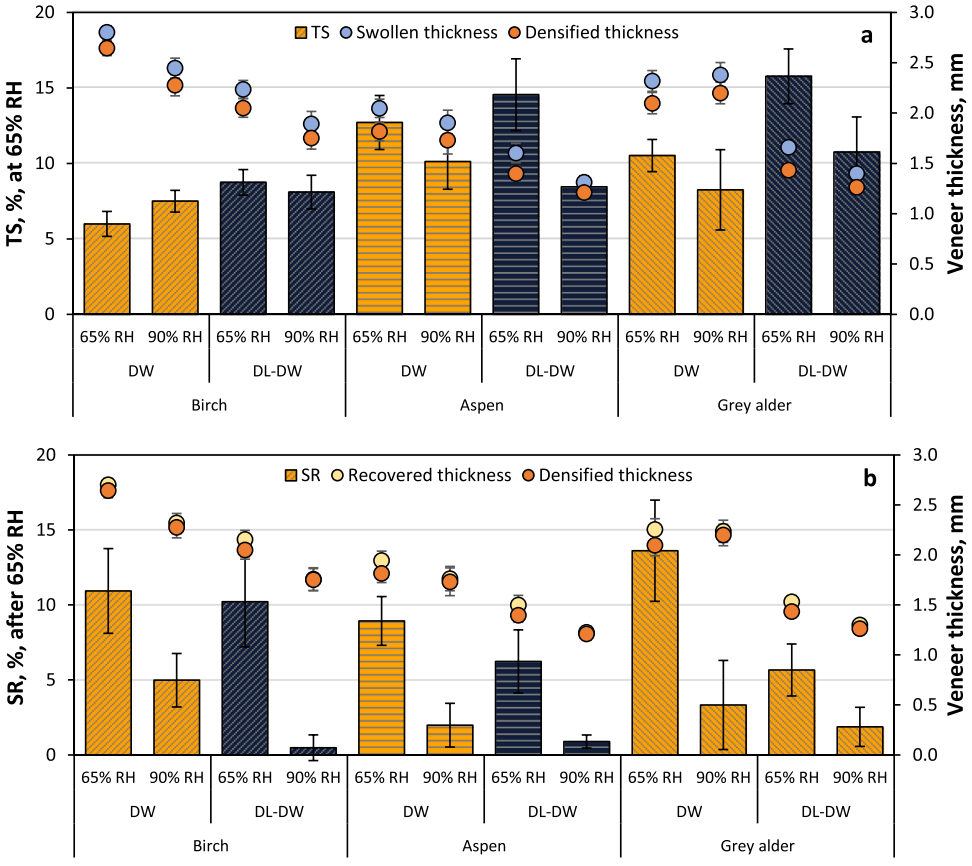


**Fig. 4.** Average (n=10) thickness swelling (TS) and set-recovery (SR) values in conjunction with swollen thickness ($T_{max}$), densified thickness ($T_d$), and recovered thickness ($T_r$) for DW and DL-DW (at 65 % and 90 % RH) samples after humid conditions of 65 % RH.

wood density was increased by 43–104 % for undelignified (DW) and 90–148 % for delignified (DL-DW) samples, compared with the respective values of 20–64 % and 42–114 % achieved at 65 % RH. It is generally observed that as the moisture content increases from 10 % to 16 %, there is a corresponding 23–30 % decrease in compressive strength perpendicular to the grain [36]. Therefore, pronounced deformation is anticipated solely from higher moisture content in wood. Additionally, wood conditioning at a higher relative humidity would lower the lignin glass transition temperature and therefore increase lignin flowability to result in a more sufficiently plasticized wood to enable microfibrils to deform independently of the surrounding matrix, in agreement with the literature [2,8,21].

In previous studies, a lower MC resulted in minimal CR and density changes when densified at 100°C. For example, Bekhta et al. [37] densified undelignified birch and alder with a lower moisture content of 5 % at 100°C and 8 MPa and achieved density increase of approximately 25 % and 50 %, respectively, each of which is only half of the respective density increases achieved in the present study of DW at 16 % MC with a pressure of only 6 MPa. This suggests that densifying the samples at a higher relative humidity leads to a greater density, thus, greater attributes. This observation was also noted by Frey et al. [38] regarding delignified wood, where samples conditioned at 95 % RH exhibited lower densification forces and higher densities compared to those conditioned at 65 % RH.

### 3.3. Microstructure of densified wood

The changes in the microstructure of wood by delignification and densification were revealed by light microscopic imaging (LM) of the cross-section of wood veneers taken from the center of the samples (Fig. 2). Since all species in this work are diffuse-porous hardwoods, the densification, in general, was fairly uniform throughout growth rings. In addition, we did not observe significantly more void volume in the center of the veneer versus the face, indicating that the specimen had similar stiffness throughout the cross-section during pressing (Fig. 2**c, d, e, f**). Overall, compression mainly occurred in vessels with buckling of ray cells and collapsing of lumens, patterns typically reported in the literature [39,40,41]. The thickness of the undelignified densified wood varied between 1.7 mm (aspen) to 2.6 mm (birch). Given that birch exhibits the highest final thickness, as previously mentioned, it is plausible that cells possessing thicker walls in relation to their lumen width are less prone to deformation [35]. The conjunction of delignification and increased relative humidity (RH) during densification results in greater deformation of the wood, leading to a reduction in thickness of the delignified veneer from 3.0 – 3.1 mm to 1.2 mm (aspen) – 1.8 mm (birch).

Given that aspen and grey alder initially exhibit similar densities, a consistent trend emerges where aspen displays a greater susceptibility to deformation. When comparing the species based on their native structure, it is notable that grey alder exhibits wider wood rays (Figs. 2 **and** 3**b**). These rays serve as reinforcement when specimens are compressed radially, leading to higher radial stiffness [42,43]. Additionally, when compared to birch, which features more visible rays than aspen but lacks the prominence seen in grey alder, it becomes evident that the narrower rays allow vessels to deform more freely (Fig. 3). Consequently, grey alder cannot achieve as much thickness reduction as aspen, which has less prominent and narrower rays.

### 3.4. Dimensional stability

#### 3.4.1. In humid conditions

The thickness swelling (TS) and set-recovery (SR) of densified wood (DW, DL-DW) were examined upon exposure to a 65 % RH environment at 25°C (Fig. 4). Sample swellings ranged from 6 % to 18 %, with the set-recovery of 1–14 %. Initially, in these conditions, water is bound between the amorphous polymers, resulting in minimal swelling [44].

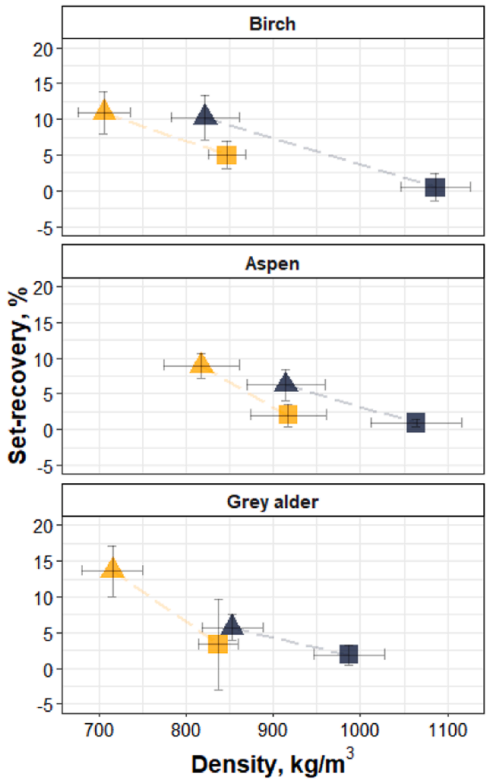


**Fig. 5.** Average (n=10) set-recovery (SR) values in humidity conditions depending on density for DW and DL-DW samples. **Yellow symbols**: DW; **Navy blue symbols**: DL-DW. **Densification conditions**: Densified at ▲▲ 65 % RH; ■■ 90 % RH.

Primarily, when viewed from a broader perspective, the delignified and densified (DL-DW) specimen exhibited greater thickness swelling (TS) in all species. However, upon closer examination based on densification parameters, a different narrative emerges. Specimens densified under a higher moisture content (MC) exhibited greater stability at the lower end of the TS and SR range, particularly noticeable in DL-DW samples. In the case of set-recovery, SR appears to be inversely correlated to wood density (Fig. 5). A higher density had a greater effect on SR which could be achieved through delignification and/or increasing MC during densification. In our study, the combination of these factors (DL-DW, compressed at 90 % RH) resulted in SR values ranging from 1 % to 2 %, while DW densified with lower moisture content led to SR values ranging from 9 % to 14 %. The lower TS and SR could stem from reduced swelling forces resulting from increasing carbohydrate polymer chain slippage, lignin flow, lower lignin stiffness, and hydrogen bond formation in delignified samples [2,33,34]. This is discussed in the literature in terms of reducing the amount of irreversible swelling caused by releasing compressive stresses [45,46], particularly evident in DL-DW samples. Increasing hydrogen bond formations between cellulose chains in delignified wood has been proposed by X. Han et al. [47] and Song et al. [31].

#### 3.4.2. In water

Although the humid environment is more typical in service, the adverse condition of immersion in water provides a clearer assessment of dimensional stability. After water immersion, all the samples returned to a thickness similar to their pre-densification water-swollen state (Fig. 6**a**). The TS of DW samples varied from 24 % to 82 % with the highest value observed in aspen densified at 90 % RH. With delignification (DL-DW), the samples showed swelling of over 100 %, peaking at 146 % for aspen densified under the same conditions. It could be correlated with the compression ratio. The facilitation of cell collapse

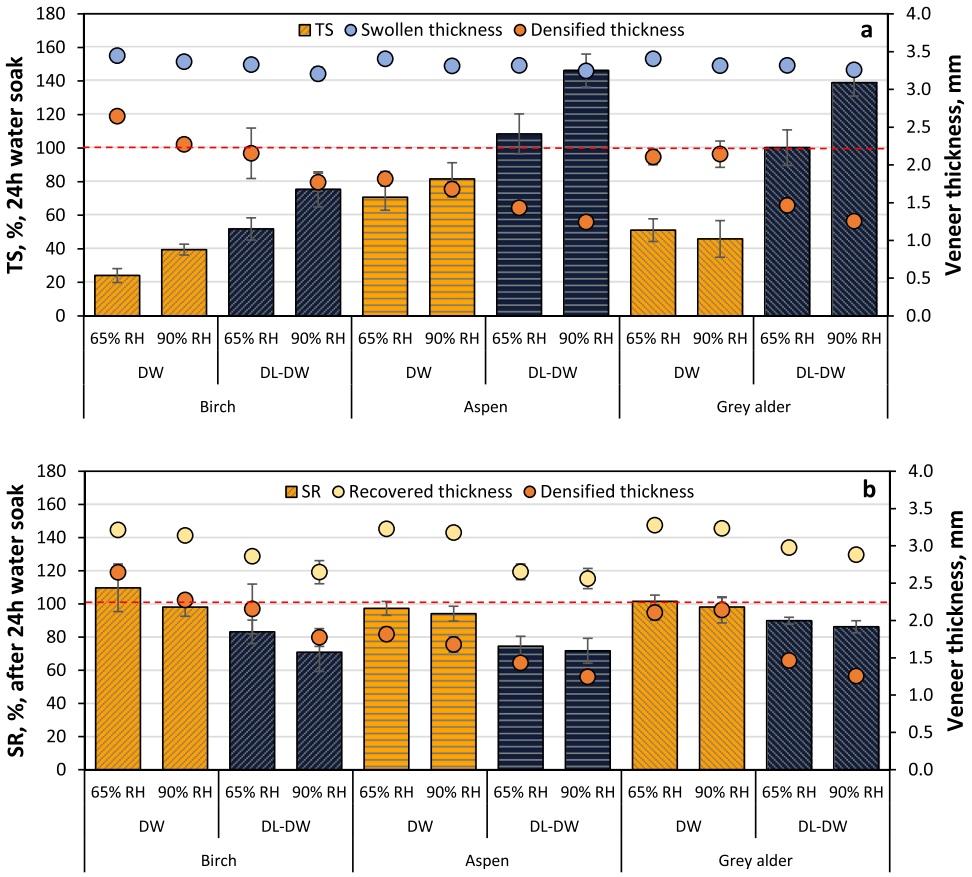


**Fig. 6.** Average (n=10) thickness swelling (TS) and set-recovery (SR) values along with swollen thickness ($T_{max}$), densified thickness ($T_d$), and recovered thickness ($T_r$) for DW and DL-DW (at 65 % and 90 % RH) samples after water immersion.

during densification is enhanced by the removal of lignin. When combined with increasing relative humidity during densification, this process yields a higher CR. Because TS is based on the difference between densified and swollen thickness, the variables will have differing baselines. Yet all the samples reached their maximum bound water capacity as their swollen thickness ranged from 3.2 to 3.5 mm, mirroring the trend of their original thickness before densification.

In the context of wood delignification methods, Jakob et al. [48] noted that organosolv delignification resulted in lower TS than alkaline delignification due to the increasing removal of hemicelluloses. In the current study, acid chlorite delignification minimized the dissolution of hemicelluloses, which offers the most accurate representation of the impact of lignin on swelling.

Even though the swollen thicknesses of all specimens were similar, DL-DW samples exhibited a greater return to their densified state after oven-drying (i.e. SR) than DW samples (Fig. 6**b**). SR of DW specimens was 94–110 % while DL-DW samples were 71–90 % ($p < 0.001$). According to Kollmann et al. [8], SR is more dependent on the internal stress in a densified specimen rather than CR. In his work, it was noted that the SR could be reduced by elevating the densification temperature, extending the pressing time, or adjusting the initial moisture content, despite all specimens achieved nearly full compression. In our investigation, we found that increasing the initial moisture content for compression improved SR, particularly when coupled with delignification. This delignification-densification approach demonstrated effectiveness across all species, particularly notable in aspen, which exhibited the highest compression ratio (60 %) and density increase (148 %), yet its SR remained one of the most desirable (72 %). This trend persists consistently across each species, indicating that DL-DW at 95 % RH yielded the highest values of density (89–148 % increase) and CR (48–60 %) within the constraints of their respective wood structures while minimizing their set-recovery to a range of 71–86 %. Hence, it seemed that the delignification, along with increasing MC in the wood, reduced stress accumulation within a specimen in agreement with previously mentioned possible mechanisms in the literature, such as enhanced chain slippage, hydrogen bonding, and lignin's flowability. Although delignification decreased SR, the lowest SR of 71 % is still relatively high, indicating that lignin likely does not have a major role in set-recovery. An alternative approach could involve employing lower-pressure densification, as it tends to result in decreasing accumulation of internal stresses compared to densification at higher pressures [49]. J. Wang et al. [40] obtained the lowest SR of 30 % with the highest degree of alkaline delignification of 35 % using poplar wood with a CR of 20 %.

### 3.4.3. Morphology of recovered samples

The microscopic images after water immersion and oven-drying are shown in Fig. 7. The thickness of undelignified (DW) samples showed complete or almost complete recovery to their initial undensified thickness (3.1–3.3 mm), regardless of species, in agreement with Laine et al. [50]. The aspens' structure is comparable to the reference, confirming the recovery (Figs. 7**a and** 7**b**) that applies to all wood species studied, including birch and grey alder.

For delignified (DL-DW) samples, it was observed that the recovered thickness after drying was 4 – 11 % lower than the initial undensified thickness (3.0–2.7 mm), indicating permanent deformation. The delignified aspen had the lowest final thickness of 2.7 mm (Fig. 7). The vessels in recovered samples did not entirely recover to their original oval shape. In addition, cell axes are more likely to be curved rather than aligned in the radial direction due to cell wall buckling and tilting during densification, in agreement with Blomberg et al. [35].

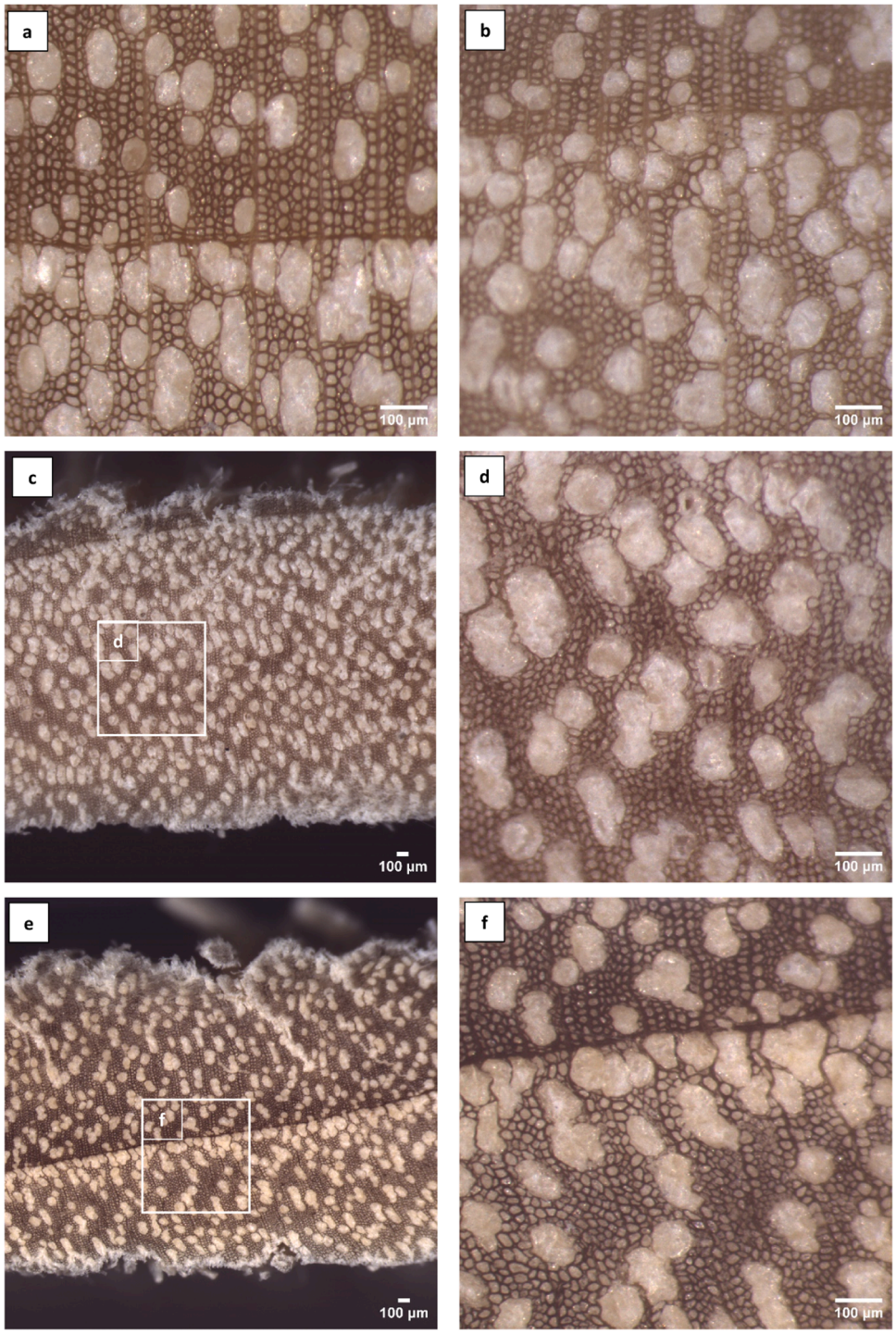


**Fig. 7.** Micrographs of densified aspen after water immersion then oven-dried: **a** - NW; **b** – DW, densified 90 % RH; **c & d** – DL-DW, densified 65 % RH; **e & f**– DL-DW, densified 90 % RH.

## 4. Conclusion

This study investigates the impact of partial lignin removal on set-recovery and densification performance. As it has been unclear whether semicrystalline cellulose or lignin had a higher impact on permanent fixation, one variable was studied at a time. To accomplish this, chlorite delignification was utilized. This focused approach assists in identifying the impacts of lignin alone, providing new insights into how it particularly contributes to dimensional stability. Partial lignin removal before densification increases the compression ratio and final density while preserving the integrity of wood cells. The densities of aspen and grey alder were increased to 1064 kg/m$^3$ and 987 kg/m$^3$ by wood delignification followed by densification, respectively, making them suitable for high-end applications. Delignification improved the dimensional stability of densified wood with lower set-recovery after humid conditions and water immersion and oven-drying compared with without delignification. Combining delignification with a higher moisture content during compression proved beneficial, reducing set-recovery from a total recovery of 100 % to as low as 70 %. One of the reasons for the reduced set-recovery could be reduced stress

accumulation during densification, while enhanced chain slippage, hydrogen bonding, and lignin flow are also possible. These findings indicate that lignin has a role in resisting cell wall deformation during densification and in driving the cell wall back to its original shape during rewetting. However, because the set-recovery of delignified wood is still 70 % or higher, lignin is unlikely to be the major contributor to set-recovery.

## CRediT authorship contribution statement

**Catherine Kilumets:** Writing – review & editing, Writing – original draft, Visualization, Methodology, Investigation, Data curation, Conceptualization. **Heikko Kallakas:** Writing – review & editing, Supervision, Funding acquisition. **Sally Ralph:** Methodology, Conceptualization. **J. Y. Zhu:** Writing – review & editing, Supervision, Conceptualization. **Christopher G. Hunt:** Writing – review & editing, Supervision, Conceptualization. **Anti Rohumaa:** Writing – review & editing, Funding acquisition. **Jaan Kers:** Writing – review & editing, Funding acquisition.

## Declaration of Generative AI and AI-assisted technologies in the writing process

During the preparation of this work, the authors used ChatGPT 3.5 in order to enhance readability and language. After using this tool, the authors reviewed and edited the content as needed and take full responsibility for the content of the publication.

## Declaration of Competing Interest

The authors declare that they have no known competing financial interests or personal relationships that could have appeared to influence the work reported in this paper.

## Acknowledgments

The authors thank Peter Kitin of the USDA Forest Service, Forest Products Laboratory, for guidance with specimen preparation for morphology, and Carlos Baez of the USDA Forest Service, Forest Products Laboratory, for conducting chemical composition analyses. This work was supported by the Estonian Research Council grant (PRG2213) and the Environmental Investment Center (MNKE22048). The authors acknowledge the Education and Youth Board for a Kristjan Jaak scholarship that made it possible for Catherine Kilumets to visit USDA Forest Service, Forest Products Laboratory.

## Data availability

Data will be made available on request.

## References

[1] J. Blomberg, B. Persson, A. Blomberg, Effects of semi-isostatic densification of wood on the variation in strength properties with density, Wood Sci. Technol. vol. 39 (5) (Aug. 2005) 339–350, https://doi.org/10.1007/S00226-005-0290-8/TABLES/5.

[2] P. Navi, F. Heger, Combined densification and thermo-hydro-mechanical processing of wood, MRS Bull. vol. 29 (5) (Jan. 2004) 332–336, https://doi.org/10.1557/MRS2004.100/METRICS.

[3] C. Tenorio, R. Moya, A. Navarro-Mora, Flooring characteristics of thermo-mechanical densified wood from three hardwood tropical species in Costa Rica, Cienc. Y. Tecnol. ía (23) (2021) 1–12, https://doi.org/10.4067/s0718-221x2021000100416.

[4] P. Bekhta, E.A. Salca, Influence of veneer densification on the shear strength and temperature behavior inside the plywood during hot press, Constr. Build. Mater. vol. 162 (Feb. 2018) 20–26, https://doi.org/10.1016/J.CONBUILDMAT.2017.11.161.

[5] K. Laine, K. Segerholm, M. Wålinder, L. Rautkari, M. Hughes, C. Lankveld, Surface densification of acetylated wood, Eur. J. Wood Wood Prod. vol. 74 (6) (Nov. 2016) 829–835, https://doi.org/10.1007/S00107-016-1077-3.

[6] S.M.H. Yahyaee, F. Dastoorian, M. Ghorbani, S.M. Zabihzadeh, Combined effect of organosolv delignification/polymerization on the set recovery of densified poplar wood, Eur. J. Wood Wood Prod. vol. 80 (2) (Apr. 2022) 367–375, https://doi.org/10.1007/S00107-021-01756-5/FIGURES/10.

[7] B. Neyses, O. Karlsson, D. Sandberg, The effect of ionic liquid and superbase pre-treatment on the spring-back, set-recovery and Brinell hardness of surface-densified Scots pine, Holzforschung vol. 74 (3) (2020) 303–312, https://doi.org/10.1515/hf-2019-0158.

[8] F.F.P. Kollmann, E.W. Kuenzi, A.J. Stamm, Princ. Wood Sci. Technol. Part 2. Wood Based Mater. (1975).

[9] A.J. Stamm, R.M. Seborg, Resin-treated, compressed wood, Trans. Am. Inst. Chem. Eng. vol. 37 (1941) 385–398 [Online]. Available: file:///C:/No DROP/DESKTOP/FPL_1268ocr.pdf.

[10] Y. Ran, D. Lu, J. Jiang, Y. Huang, W. Wang, J. Cao, Deep eutectic solvents-assisted wood densification: a promising strategy for shape-fixation, Chem. Eng. J. vol. 471 (Sep. 2023) 144476, https://doi.org/10.1016/J.CEJ.2023.144476.

[11] C.A.S. Hill, Wood Modification: Chemical, Thermal and Other Processes, John Wiley & Sons Ltd, 2006, https://doi.org/10.1002/0470021748.

[12] T. Ding, L. Gu, X. Liu, Influence of steam pressure on chemical changes of heat-treated Mongolian pine wood, Bioresources vol. 6 (2) (Apr. 2011) 1880–1889. ⟨https://jtatm.textiles.ncsu.edu/index.php/BioRes/article/view/BioRes_06_2_1880_Ding_GL_Steam_Pressure_Chem_Changes_Pine_Wood⟩. Accessed: Oct. 31, 2023. [Online]. Available.

[13] M. Inoue, M. Norimoto, M. Tanahashi, R.M. Rowell, Steam or heat fixation of compressed wood, Wood Fiber Sci. vol. 25 (3) (1993) 224–235.

[14] L. Han, A. Kutnar, J. Couceiro, D. Sandberg, Creep properties of densified wood in bending, For. 2022, Vol. 13, Page 757 vol. 13 (5) (May 2022) 757, https://doi.org/10.3390/F13050757.

[15] B.M. Esteves, H.M. Pereira, Wood modification by heat treatment: a review, Bioresources vol. 4 (1) (Dec. 2008) 370–404, https://doi.org/10.15376/BIORES.4.1.370-404.

[16] E. Xiang, S. Feng, S. Yang, R. Huang, Sandwich compression of wood: effect of superheated steam treatment on sandwich compression fixation and its mechanisms, Wood Sci. Technol. vol. 54 (6) (Nov. 2020) 1529–1549, https://doi.org/10.1007/S00226-020-01237-7/FIGURES/10.

[17] T. Higashihara, T. Morooka, M. Norimoto, Permanent fixation of transversely compressed wood by steaming and its mechanism, Mokuzai Gakkaishi/J. Jpn. Wood Res. Soc. vol. 46 (4) (2000) 291–297.

[18] A. Lisý, A. Ház, R. Nadányi, M. Jablonský, I. Šurina, About hydrophobicity of lignin: A review of selected chemical methods for lignin valorisation in biopolymer production, Energies vol. 15 (17) (2022), https://doi.org/10.3390/en15176213.

[19] G. Sivasankarapillai, H. Li, A.G. McDonald, Lignin-based triple shape memory polymers, Biomacromolecules vol. 16 (9) (Sep. 2015) 2735–2742, https://doi.org/10.1021/ACS.BIOMAC.5B00655/ASSET/IMAGES/LARGE/BM-2015-006559_0013.JPEG.

[20] N. Plaza, S.L. Zelinka, D.S. Stone, and J.E. Jakes, Plant-based torsional actuator with memory, 2013, doi: 10.1088/0964-1726/22/7/072001.

[21] R. Seborg, M. Millet, A. Stamm, Heat-stabilized compressed wood (Staypak), Mech. Eng. vol. 67 (1) (1956) 25–31.

[22] D. Fengel, G. Wegener, Wood: Chemistry, Ultrastructure, Reactions, New York: Walter de Gruyter, 1984.

[23] T.K. Kwei, The effect of hydrogen bonding on the glass transition temperatures of polymer mixtures, J. Polym. Sci. Lett. Ed. vol. 22 (1) (1984) 307–313, https://doi.org/10.1002/pol.1984.130220603.

[24] S.S. Kelley, T.G. Rials, W.G. Glasser, Relaxation behaviour of the amorphous components of wood, J. Mater. Sci. vol. 22 (2) (1987) 617–624, https://doi.org/10.1007/BF01160778.

[25] J.E. Jakes, C.G. Hunt, S.L. Zelinka, P.N. Ciesielski, N.Z. Plaza, Effects of moisture on diffusion in unmodified wood cell walls: a phenomenological polymer science approach, Forests vol. 10 (12) (2019), https://doi.org/10.3390/F10121084.

[26] H. Kallakas, A. Rohumaa, H. Vahermets, J. Kers, Effect of different hardwood species and lay-up schemes on the mechanical properties of plywood, For. 2020, Vol. 11, Page 649 vol. 11 (6) (Jun. 2020) 649, https://doi.org/10.3390/F11060649.

[27] P.A. Ahlgren, D.A.I. Goring, Removal of wood components during chlorite delignification of black spruce, Can. J. Chem. vol. 49 (8) (1971) 1272–1275, https://doi.org/10.1139/v71-207.

[28] A. Sluiter et al., Determination of Structural Carbohydrates and Lignin in Biomass: Laboratory Analytical Procedure (LAP) (Revised July 2011), 2008, Accessed: Dec. 28, 2023. [Online]. Available: ⟨http://www.nrel.gov/biomass/analytical_procedures.html⟩.

[29] M.W. Davis, A rapid modified method for compositional carbohydrate analysis of lignocellulosics by high pH anion-exchange chromatography with pulsed amperometric detection (HPAEC/PAD), J. Wood Chem. Technol. vol. 18 (2) (1998) 235–252, https://doi.org/10.1080/02773819809349579.

[30] P. Navi, F. Girardet, Effects of thermo-hydro-mechanical treatment on the structure and properties of wood, Holzforschung vol. 54 (3) (2000) 287–293, https://doi.org/10.1515/HF.2000.048.

[31] J. Song, et al., Processing bulk natural wood into a high-performance structural material, Nat. 2018 554:7691 vol. 554 (7691) (Feb. 2018) 224–228, https://doi.org/10.1038/nature25476.

[32] M.I. Shams, H. Yano, K. Endou, Compressive deformation of wood impregnated with low molecular weight phenol formaldehyde (PF) resin III: effects of sodium chlorite treatment, J. Wood Sci. vol. 51 (3) (2005) 234–238, https://doi.org/10.1007/s10086-004-0638-y.

[33] T. Yang, J. Cao, C. Mei, E. Ma, Effects of chlorite delignification on dynamic mechanical performances and dynamic sorption behavior of wood, Cellulose vol. 28 (14) (Sep. 2021) 9461–9474, https://doi.org/10.1007/S10570-021-04137-6/FIGURES/9.
[34] M. Frey, et al., Tunable wood by reversible interlocking and bioinspired mechanical gradients, Adv. Sci. vol. 6 (10) (May 2019), https://doi.org/10.1002/ADVS.201802190.
[35] J. Blomberg, B. Persson, U. Bexell, Effects of semi-isostatic densification on anatomy and cell-shape recovery on soaking, Holzforschung vol. 60 (3) (May 2006) 322–331, https://doi.org/10.1515/HF.2006.052/MACHINEREADABLECITATION/RIS.
[36] U. Forest Service and F. Products Laboratory, Wood Handbook, Wood as an Engineering Material, 2010, Accessed: Mar. 27, 2024. [Online]. Available: ⟨www.fpl.fs.fed.us⟩.
[37] P. Bekhta, S. Proszyk, T. Krystofiak, J. Sedliacik, I. Novak, M. Mamonova, Effects of short-term thermomechanical densification on the structure and properties of wood veneers, Jan vol. 12 (1) (2015) 40–54, https://doi.org/10.1080/17480272.2015.1009488. ⟨https://doi.org/10.1080/17480272.2015.1009488⟩.
[38] M. Frey, D. Widner, J.S. Segmehl, K. Casdorff, T. Keplinger, I. Burgert, Delignified and densified cellulose bulk materials with excellent tensile properties for sustainable engineering, ACS Appl. Mater. Interfaces vol. 10 (5) (Feb. 2018) 5030–5037, https://doi.org/10.1021/ACSAMI.7B18646/ASSET/IMAGES/LARGE/AM-2017-186465_0008.JPEG.
[39] G. Standfest, A. Kutnar, B. Plank, A. Petutschnigg, F.A. Kamke, M. Dunky, Microstructure of viscoelastic thermal compressed (VTC) wood using computed microtomography, Wood Sci. Technol. vol. 47 (1) (Jan. 2013) 121–139, https://doi.org/10.1007/S00226-012-0496-5/FIGURES/6.
[40] J. Wang, J. Liu, J. Li, J.Y. Zhu, Characterization of microstructure, chemical, and physical properties of delignified and densified poplar wood, Materials vol. 14 (19) (Oct. 2021), https://doi.org/10.3390/MA14195709.
[41] J. Wang, S.J. Fishwild, M. Begel, J.Y. Zhu, Properties of densified poplar wood through partial delignification with alkali and acid pretreatment, J. Mater. Sci. vol. 55 (29) (Oct. 2020) 14664–14676, https://doi.org/10.1007/S10853-020-05034-2/FIGURES/6.
[42] M. Jakob, W. Gindl-Altmutter, The effect of partial delignification on the stress–strain relationship in transverse compression, J. Mater. Sci. vol. 58 (3) (Jan. 2023) 1071–1085, https://doi.org/10.1007/S10853-022-08074-Y/FIGURES/11.
[43] A. Cloutier, et al., The effect of rays on the mechanical behaviour of beech and birch at different moisture and temperature conditions perpendicular to the grain, For. 2024, Vol. 15, Page 584 vol. 15 (4) (Mar. 2024) 584, https://doi.org/10.3390/F15040584.
[44] N.Z. Plaza, S.V. Pingali, S. Qian, W.T. Heller, J.E. Jakes, Informing the improvement of forest products durability using small angle neutron scattering, Cellulose vol. 23 (3) (Jun. 2016) 1593–1607, https://doi.org/10.1007/S10570-016-0933-Y/FIGURES/8.
[45] L.M. Arruda, C.H.S. Del Menezzi, Effect of thermomechanical treatment on physical properties of wood veneers, Int. Wood Prod. J. vol. 4 (4) (Nov. 2013) 217–224, https://doi.org/10.1179/2042645312Y.0000000022.
[46] C.H. Fang, N. Mariotti, A. Cloutier, A. Koubaa, P. Blanchet, Densification of wood veneers by compression combined with heat and steam, Eur. J. Wood Wood Prod. vol. 70 (1–3) (Jan. 2012) 155–163, https://doi.org/10.1007/S00107-011-0524-4/FIGURES/12.
[47] X. Han, Y. Ye, F. Lam, J. Pu, F. Jiang, Hydrogen-bonding-induced assembly of aligned cellulose nanofibers into ultrastrong and tough bulk materials, J. Mater. Chem. A Mater. vol. 7 (47) (Dec. 2019) 27023–27031, https://doi.org/10.1039/C9TA11118B.
[48] M. Jakob, G. Stemmer, I. Czabany, U. Müller, W. Gindl-Altmutter, Preparation of high strength plywood from partially delignified densified wood, Polym. 2020, Vol. 12, Page 1796 vol. 12 (8) (Aug. 2020) 1796, https://doi.org/10.3390/POLYM12081796.
[49] A. Darwis, I. Wahyudi, W. Dwianto, T.D. Cahyono, Densified wood anatomical structure and the effect of heat treatment on the recovery of set, J. Indian Acad. Wood Sci. vol. 14 (1) (Jun. 2017) 24–31, https://doi.org/10.1007/S13196-017-0184-Z/FIGURES/5.
[50] K. Laine, et al., Micromorphological studies of surface densified wood, J. Mater. Sci. vol. 49 (5) (2014) 2027–2034, https://doi.org/10.1007/s10853-013-7890-8.